Cell Metabolism

Supplemental Information

The LYR factors SDHAF1 and SDHAF3 mediate maturation of the iron-sulfur subunit of succinate dehydrogenase

Un Na, Wendou Yu, James Cox, Daniel K. Bricker, Knut Brockmann, Jared Rutter, Carl S. Thummel and Dennis R. Winge

Figure S1. Related to Figure 1. Cell lacking Sdh6 or Sdh7 exhibit respiratory growth defects and SDH deficiency

(A) Respiratory growth defects of *sdh6*Δ and *sdh7*Δ mutants are complemented by exogenously expressed epitope-tagged Sdh6 and Sdh7, respectively. Low-copy plasmids with either *MET25* promoter for His_6-2Myc or own endogenous promoters for His_6-3HA were transformed. 10-fold dilutions starting from OD_{600}=0.5 were spotted on synthetic complete media containing carbon sources indicnated, and then incubated at 30°C. (B) SDH and bc_1 Complex III activity in *sdh6*Δ mutants, *sdh7*Δ mutants and *sdh6*Δ *sdh7*Δ double mutants from mid-log cultures. Data are represented as mean ± SD (N=3; ns, not significant; **$p < 0.05$). (C) Relative pyruvate dehydrogenase (PDH) activity, α-ketoglutarate dehydrogenase (α-KGDH) activity and malate dehydrogenase (MDH) activity in mitochondria from late-log phase cells lacking Sdh6 or Sdh7. Data are represented as mean ± SD (N=3).

Figure S1

A

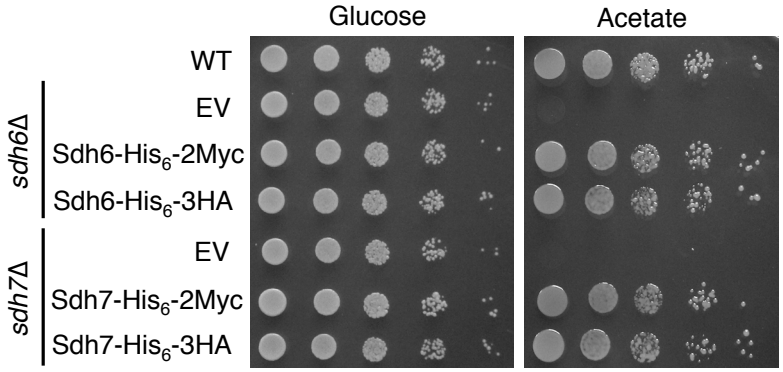

B

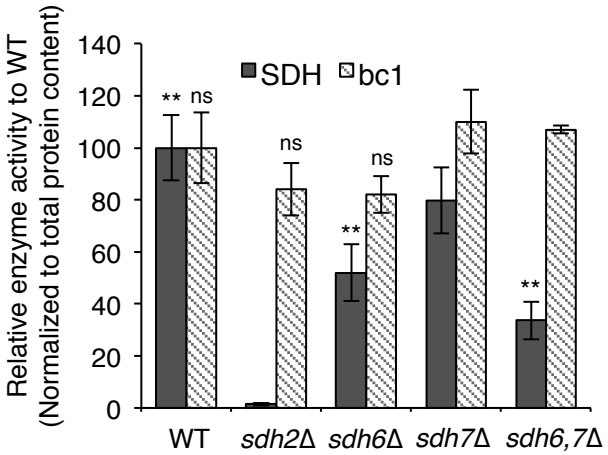

C

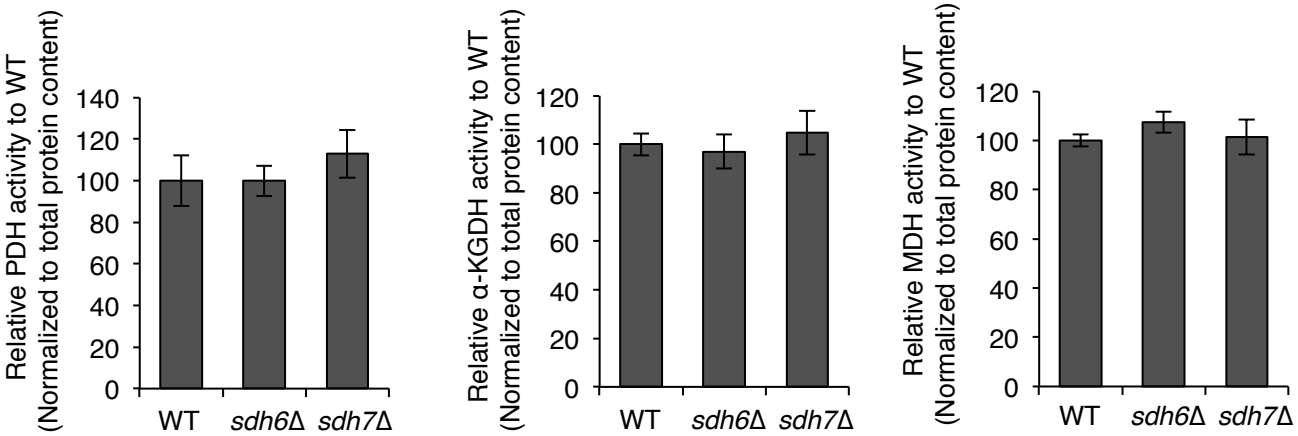

Figure S2. Related to Figure 1. BN-PAGE analysis of respiratory complexes

Mitochondria from the strains were solubilized with 1% digitonin. Soluble fractions were separated on BN-PAGE and transferred to membranes for detection of protein complexes using appropriate antibodies. Sdh1, a subunit of SDH; F1β, a subunit of Complex V. The band highlighted by ** is the Sdh1 assembly intermediate

Figure S2

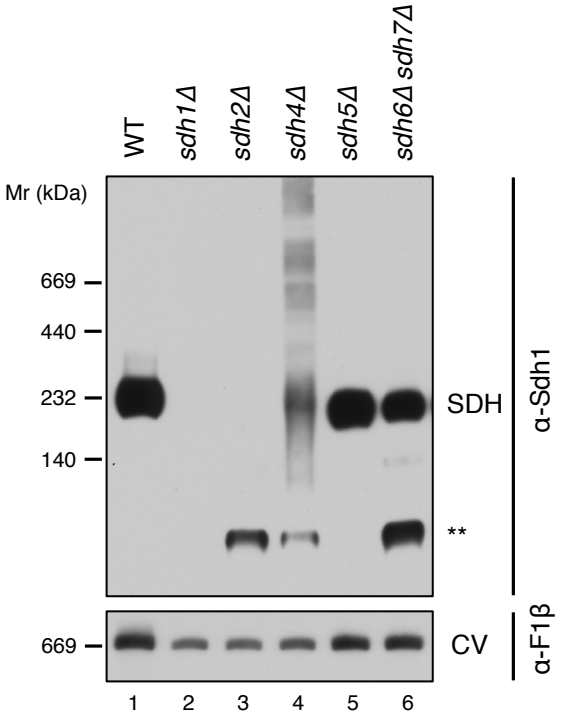
WT
sdh1Δ
sdh2Δ
sdh4Δ
sdh5Δ
sdh6Δ sdh7Δ
Mr (kDa)
669
440
232
140
SDH
**
α-Sdh1
669
CV
α-F1β
1
2
3
4
5
6

Figure S3. Related to Figure 2. SDH subunit steady-state levels, Sdh6-His$_6$-2Myc co-immunoprecipitation and Sdh7 suborganellar localization

(A) Steady-state levels of SDH subunits in cells lacking each SDH subunit. (B) Mitochondrial lysates were obtained after solubilization with 1% digitonin, which were subjected to anti-Myc antibody-conjugated magnetic beads. Bound substances to Myc antibody beads were resolved on SDS-PAGE and detected by immunoblotting. Input, 4% of total lysates. (C) Proteinase K assay to assess the localization of Sdh7. Sdh7-Myc was expressed in *sdh7*Δ mutants and mitochondria were isolated. Intact mitochodria, hyoptonic buffer treated mitochondria and 1% Triton X-100 treated mitochondria were incubated with proteinase K for 30 min on ice. Sample were resolved on SDS-PAGE. Aco1, a soluble mitochondrial matrix protein; Mia40, a mitochondrial intermembrane space protein.

Figure S3

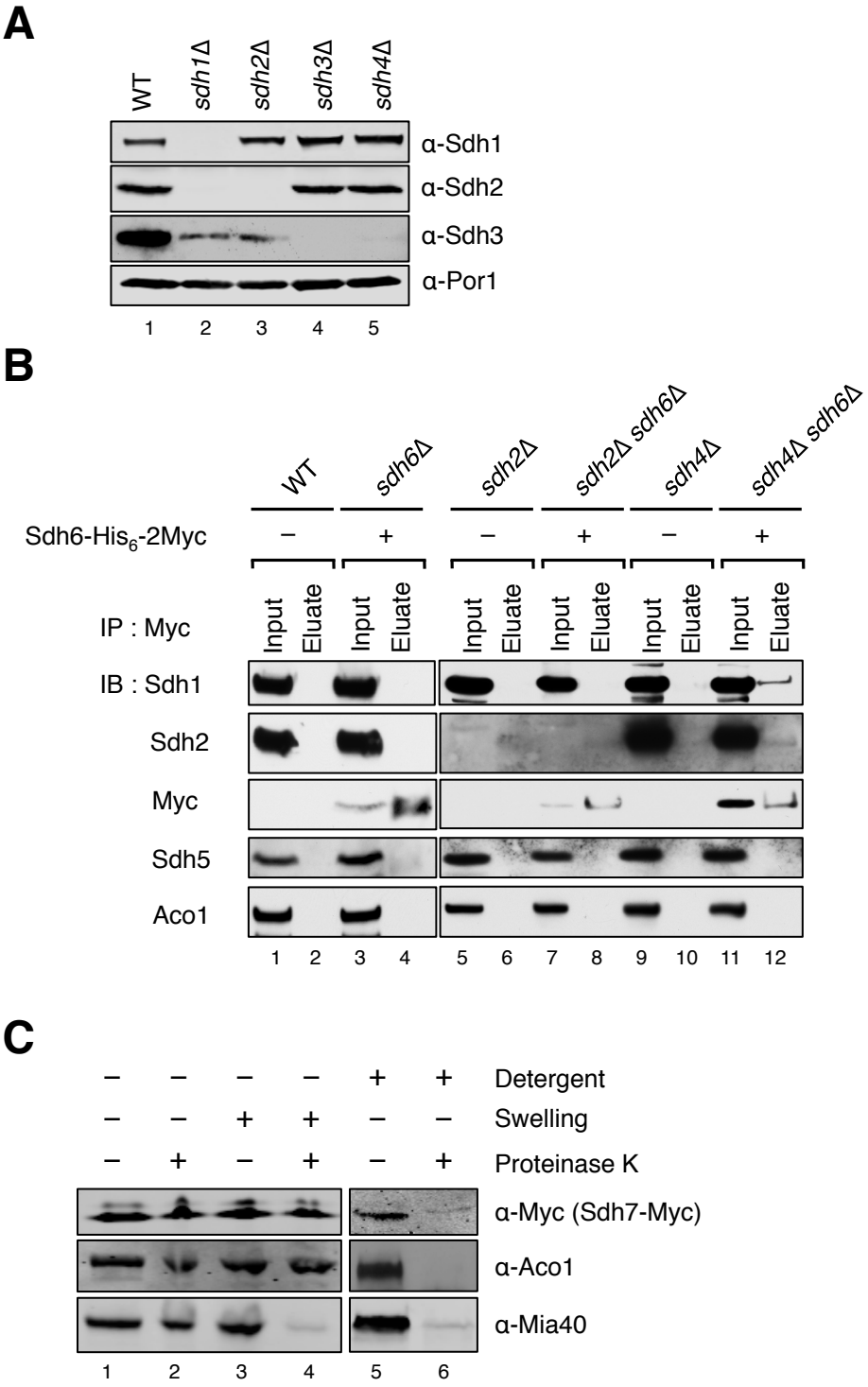
A
WT
sdh1Δ
sdh2Δ
sdh3Δ
sdh4Δ
α-Sdh1
α-Sdh2
α-Sdh3
α-Por1
1 2 3 4 5
B
WT
sdh6Δ
sdh2Δ
sdh2Δ sdh6Δ
sdh4Δ
sdh4Δ sdh6Δ
Sdh6-His6-2Myc
− + − + − +
IP : Myc
Input Eluate Input Eluate Input Eluate Input Eluate Input Eluate Input Eluate
IB : Sdh1
Sdh2
Myc
Sdh5
Aco1
1 2 3 4 5 6 7 8 9 10 11 12
C
− − − − + + Detergent
− − + + − − Swelling
− + − + − + Proteinase K
α-Myc (Sdh7-Myc)
α-Aco1
α-Mia40
1 2 3 4 5 6

Figure S4. Related to Figure 2. Genetic and biochemical approaches to elucidate detailed mechanisms by which Sdh6 and Sdh7 play roles in Sdh2 maturation

(A) Cells harboring either high-copy *SDH2* plasmid or empty vector (EV) were spotted on synthetic complete media by 10-fold serial dilutions, and incubated at 30°C. (B) Steady-state levels of Sdh2 overexpressed. (C) Cells harboring both high-copy *SDH3* plasmids and *SDH4* plasmids were spotted on synthetic complete media by 10-fold serial dilutions, and incubated at 30°C. (D) Steady-state levels of Sdh2 upon overexpression of Sdh3 and Sdh4 in *sdh6*Δ and *sdh7*Δ mutants. (E) ^{55}Fe incorporation into ectopically expressed Sdh2-His$_6$-2Myc in cells lacking Sdh6 or Sdh7 was measured. Pre-cultured cells in iron-free media were incubated with ^{55}Fe for 2 hours for *in vivo* labeling in the presence of 1 mM sodium ascorbate that is essential for efficient iron uptake. This assay was done as described previously (Molik et al., 2007). Co-immunoprecipitation was performed with whole cell lysates. This assay was carried out with *sdh4*Δ background where a Sdh1/Sdh2 subcomplex accumulates. The chart is shown as mean ± SD from three independent experiments. (Notes: as described in the main text, this experiment has numerous caveats. Ascorbate may mimic the exogenous reductants in suppressing the defects in the mutant cells. Also, since Sdh2 contains 3 distinct FeS clusters containing 9 Fe atoms in total, the observed lack of diminution in ^{55}Fe labeling in mutant cells does not reveal whether Sdh6 or Sdh7 have a specialized role with one FeS cluster type.)

Figure S4

A

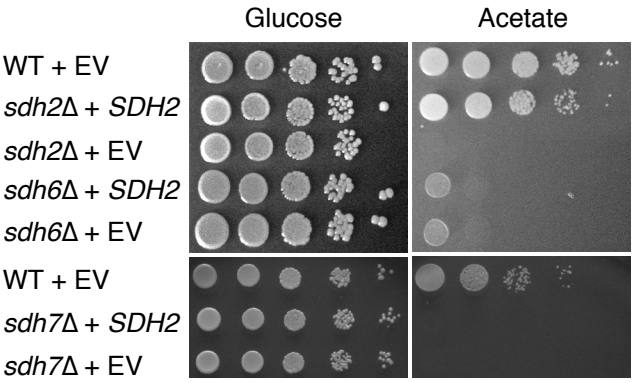

B

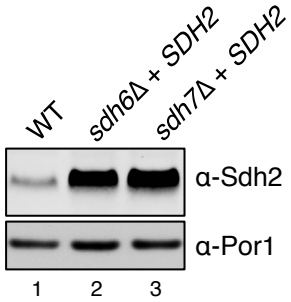

C

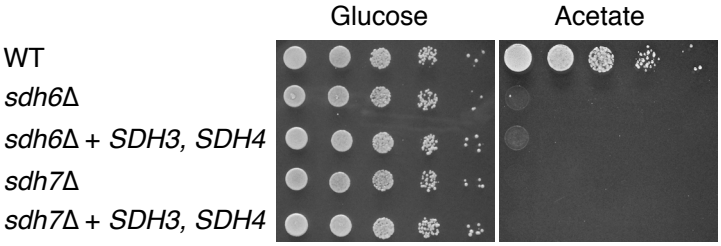

D

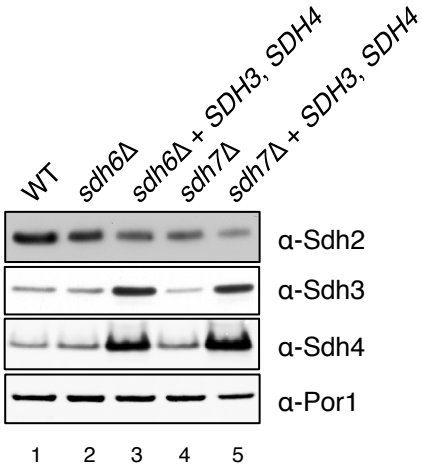

E

^{55}Fe incorporation into Sdh2-His$_6$-2Myc (cpm/g cells)

	Replicate 1	Replicate 2	Replicate 3
sdh4Δ	420	284	226
sdh4Δ sdh6Δ	272	280	262
sdh4Δ sdh7Δ	652	348	250

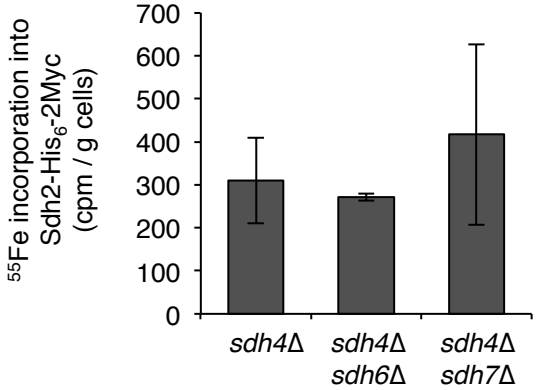

Figure S5. Related to Figure 5. Generation and characterization of *dSdhaf3* null mutants

(A) Amino acid sequence alignment of Sdh7 orthologs in eukaryotes using Clustal Omega. (B) Gene targeting was used to disrupt the *dSdhaf3* locus. A *miniwhite* selectable marker was flanked by two 3 kb regions of homology to the *dSdhaf3* locus (5'HA and 3'HA), resulting in the deletion of 339 bp of *dSdhaf3* coding region upon homologous recombination. (C) The structure of the mutated *dSdhaf3* locus was confirmed by Southern blot hybridization. Genomic DNA was isolated from three genetic backgrounds: (1) w^{1118} control flies, (2) two independent transformant lines that carry the *dSdhaf3* targeting construct integrated randomly in the genome (donor strains 1 and 2), and (3) the *dSdhaf3* deletion mutant generated using donor strain #2 (see Supplemental Experimental Procedures). The DNA was cut using *HindII* and *EcoRV* restriction endonucleases and analyzed by Southern blot hybridization using probes to detect the 5' and 3' regions of the dSdhaf3 locus. These probes will detect a 2.8 kb fragment from the wild-type locus, and 0.73 and 3.4 kb fragments from the disrupted gene containing the miniwhite marker. The Southern blot shows that only the 2.8 kb fragment is present in the w^{1118} control, as expected (lane 1). The two donor strains carry both the wild-type locus and the 3.4 kb and 0.73 kb fragments from the targeting construct (lanes 2,3). The homozygous *dSdhaf3* mutant has only the 3.4 kb and 0.73 kb fragments, as expected (lane 4). Note that the ~7 kb fragment in donor strain #1 is of unknown origin. Donor strain #2 was used to generate the *dSdhaf3* mutant used in this study. (D) GC/MS was used to compare the relative levels of small metabolites in wild-type controls (grey boxes) and *dSdhaf3* mutants (white boxes). N=12 samples from two

independent experiments with 20 flies/sample (5-day old). ***p<0.001. (E) Proteins from purified mitochondria were extracted from w^{1118} controls (+) and *dSdhaf3* mutants (–), fractionated by non-denaturing PAGE, and analyzed for total protein by Commassie Blue staining or for flavinylated SdhA. A SdhA marker is included as a control (M). (F) Control w^{1118} flies and *dSdhaf3* mutants were tested for paralysis as described in Supplemental Experimental Procedures, scoring for the number of flies that moved off the bottom of the vial after vortexing. Results are from three independent experiments using a total of 12 vials with 20 adults/vial at 1, 2, 3, or 4-weeks of age. ***p<0.001

Figure S5

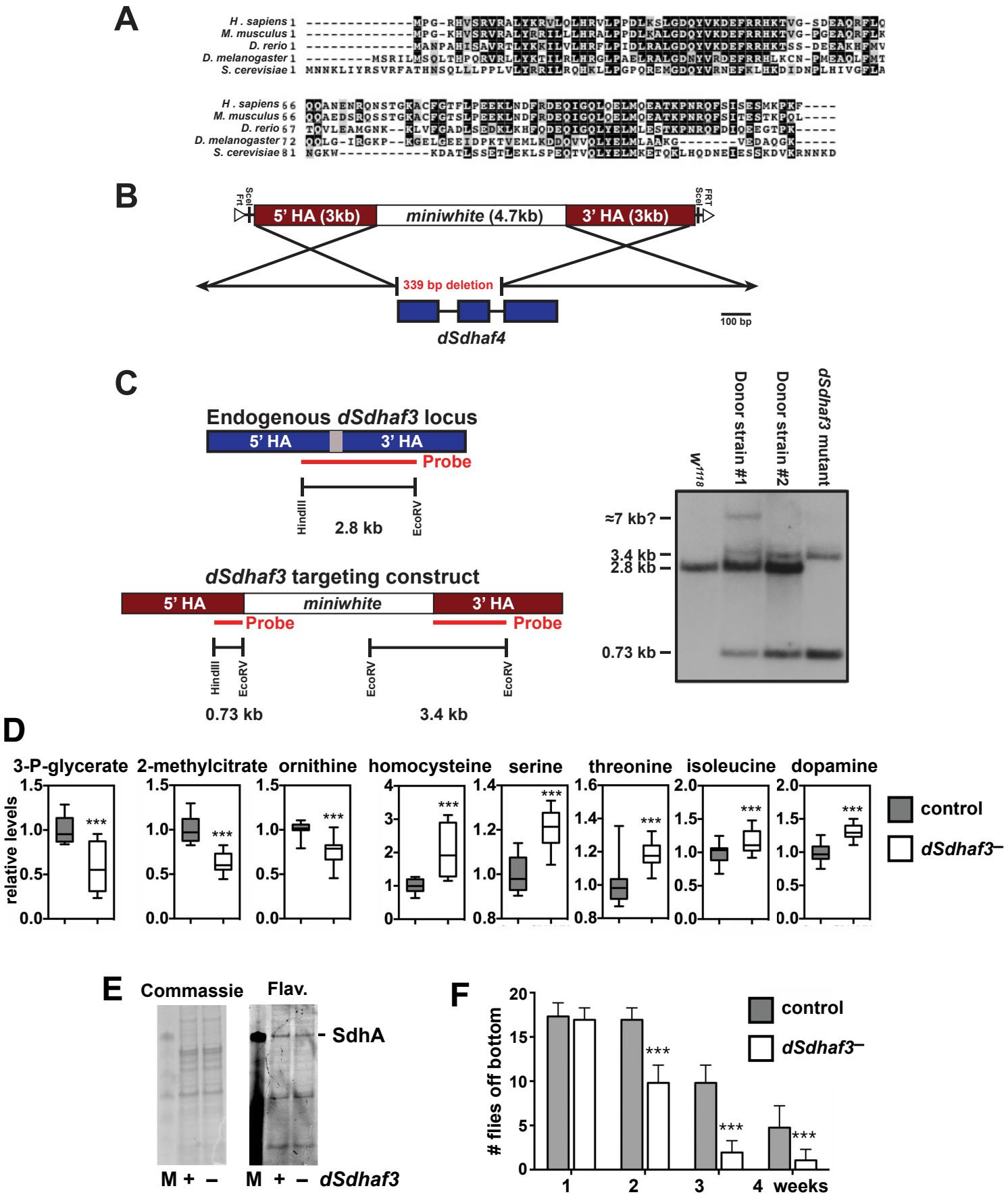
A
H. sapiens
M. musculus
D. rerio
D. melanogaster
S. cerevisiae
B
5' HA (3kb)
miniwhite (4.7kb)
3' HA (3kb)
FRT
SceI
339 bp deletion
100 bp
dSdhaf4
C
Endogenous dSdhaf3 locus
5' HA
3' HA
Probe
HindIII
2.8 kb
EcoRV
dSdhaf3 targeting construct
5' HA
miniwhite
3' HA
Probe
Probe
HindIII
EcoRV
EcoRV
EcoRV
0.73 kb
3.4 kb
w1118
Donor strain #1
Donor strain #2
dSdhaf3 mutant
≈7 kb?
3.4 kb
2.8 kb
0.73 kb
D
3-P-glycerate
2-methylcitrate
ornithine
homocysteine
serine
threonine
isoleucine
dopamine
relative levels
control
dSdhaf3−
E
Commassie
Flav.
SdhA
M + −
M + − dSdhaf3
F
flies off bottom
control
dSdhaf3−
1
2
3
4 weeks

Figure S6. Related to Figure 6. *dSdhaf3* interacts with *SdhB* and overexpression of *CG34229* fails to rescue the hyperoxia sensitivity of *dSdhaf3* mutants

(A) Flies carrying either control or *dSdhaf3* mutant chromosomes over a balancer chromosome were crossed to flies carrying a hypomorphic allele for SdhB over a balancer. The resulting progeny were scored for the absence or presence of the marker linked to the balancer chromosome. The proportion of the expected progeny that eclosed, based on Mendelian ratios of the indicated genotypes, is shown. "+" represents a *TM3* balancer for *dSdhaf3* and a *CyO* balancer for $SdhB^{12081}$. (N) = number of progeny assayed from each cross in a total of four independent experiments. The mean ± SEM is shown and ***$p<0.001$ (B) A BLAST search for a *Drosophila* Sdh6 homolog identified CG34229, which shares limited sequence similarity with both the yeast protein and human LYR proteins. Widespread overexpression of *CG34229* using *Act5C-GAL4* to drive a *UAS-CG34229* transgene in *dSdhaf3* mutants (orange line), however, had no effect on their sensitivity to hyperoxia. We conclude that the functional interaction between Sdh6 and Sdh7 may not be conserved through evolution or that the true *Drosophila* homolog of Sdh6 remains to be discovered.

Figure S6

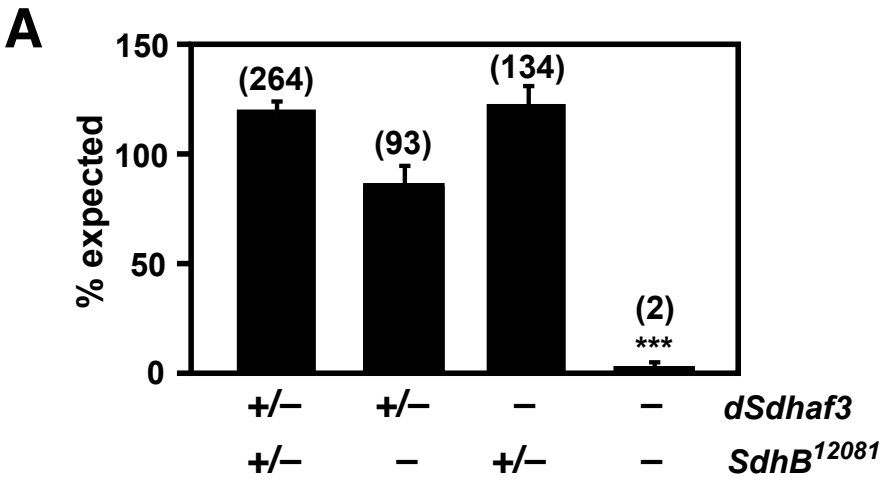
A
150
100
50
0
% expected
(264)
(93)
(134)
(2)
***
+/–
+/–
–
–
dSdhaf3
+/–
–
+/–
–
SdhB12081

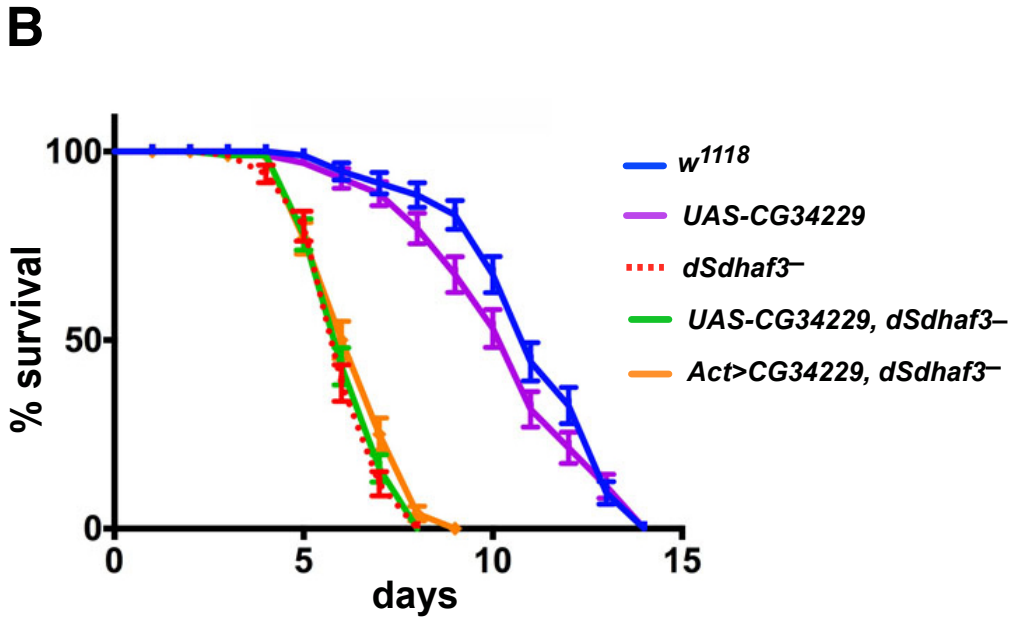
B
100
50
0
% survival
0
5
10
15
days
w1118
UAS-CG34229
dSdhaf3–
UAS-CG34229, dSdhaf3–
Act>CG34229, dSdhaf3–